

GENESIS OF CORDIERITE – GEDRITE GNEISSES, CENTRAL METASEDIMENTARY BELT BOUNDARY THRUST ZONE, GRENVILLE PROVINCE, ONTARIO, CANADA

WILLIAM H. PECK[§] AND JOHN W. VALLEY

*Department of Geology and Geophysics, University of Wisconsin, 1215 West Dayton Street,
Madison, Wisconsin 53706, U.S.A.*

ABSTRACT

Cordierite- and gedrite-bearing lithologies crop out along the base of the Central Metasedimentary Belt boundary thrust zone (CMBbtz) in Ontario, the boundary between the Central Metasedimentary Belt and the Central Gneiss Belt. It has been proposed that these rocks represent metamorphosed and partially melted Al- and Mg-rich sedimentary rocks. Whole-rock oxygen isotope values ($\delta^{18}\text{O}$ in the range 6–8‰) from these rocks are not consistent with closed-system metamorphism of either soils or pelitic sediments, and cannot be explained solely by extraction of partial melt from pelitic rocks. The whole-rock $\delta^{18}\text{O}$ and chemical composition of cordierite–gedrite rocks in the CMBbtz indicate that these rocks represent volcanic rocks hydrothermally altered by seawater. After hydrothermal alteration, these rocks were metamorphosed to the upper amphibolite facies, stabilizing the cordierite + gedrite assemblages. Diffusion modeling of quartz–garnet fractionations suggests intermineral exchange of oxygen in a closed system at moderate fugacity of H_2O during slow cooling after regional metamorphism. We believe that cordierite–gedrite lithologies in the CMBbtz mark the site of Mid-Proterozoic rifting at the margin of Laurentia.

Keywords: cordierite, gedrite, hydrothermal alteration, oxygen isotopes, Grenville Province, Fishtail Lake, Ontario.

SOMMAIRE

On trouve des roches métamorphiques à cordierite et à gédrite à la base de la zone de chevauchement qui marque la limite de la Ceinture Métasédimentaire Centrale et son contact avec la Ceinture Gneissique Centrale en Ontario. La proposition a été faite que ces roches représentent des unités alumineuses et magnésiennes métamorphosées et partiellement fondues. Les rapports d'isotopes d'oxygène déterminés sur roche totale ($\delta^{18}\text{O}$ dans l'intervalle 6–8‰) montrent une incompatibilité avec l'hypothèse d'un métamorphisme en système fermé, soit de sols ou de roches métasédimentaires pélitiques, et ne pourraient résulter de la seule extraction d'un liquide anatectique à partir de roches pélitiques. Ces rapports $\delta^{18}\text{O}$ sur roche totale et la composition chimique des roches à cordierite–gédrite font penser qu'il s'agit de roches volcaniques altérées par voie hydrothermale en présence de l'eau de mer. Après le stade d'altération, ces roches ont été métamorphosées jusqu'au faciès amphibolite supérieur, ce qui a stabilisé l'assemblage cordierite + gédrite. Un modèle de diffusion du fractionnement entre quartz et grenat nous incite à proposer un échange interminéral des isotopes d'oxygène en système fermé à fugacité moyenne de H_2O au cours d'un lent refroidissement suite au métamorphisme régional. À notre avis, les roches à cordierite–gédrite de cette transition entre socles marquent le site d'une zone extensionnelle d'âge mésoproterozoïque en marge du socle de Laurentia.

(Traduit par la Rédaction)

Mots-clés: cordierite, gédrite, altération hydrothermale, isotopes d'oxygène, Province du Grenville, lac Fishtail, Ontario.

INTRODUCTION

The low-variance mineral assemblages of cordierite – orthoamphibole (anthophyllite or gedrite) rocks have made this relatively rare rock-type the focus of numerous petrological studies (Robinson *et al.* 1982). The rarity of this lithology is caused by its unusually Mg- and Al-rich and low-Ca bulk composition, which does not have equivalents in common sedimentary, igneous, or metamorphic rocks (Seki 1957). Early investigators

attributed these chemical characteristics to a number of disparate processes including metasomatism during regional or contact metamorphism, depletion of alkalis from a pelite by melt extraction (leaving a restite enriched in Mg and Al), and metamorphism of a soil horizon or Mg-rich evaporitic sediments (Robinson *et al.* 1982).

It was recognized by Vallance (1967) that cordierite – orthoamphibole rocks from Yalwa (New South Wales, Australia) are stratigraphically equivalent to and have

[§] E-mail address: william@geology.wisc.edu

the same bulk composition as lower-grade quartz – chlorite lithologies, which are interpreted to be hydrothermally altered Devonian mafic volcanic rocks. This model explains the common association of cordierite – orthoamphibole rocks with the extensively altered stockwork zones of amphibolite-facies volcanogenic massive sulfide (VMS) deposits (*e.g.*, Bachinski 1978).

Detailed field, geochemical, and isotopic studies have documented a hydrothermally altered volcanic protolith in the case of many early Archean to Phanerozoic cordierite – orthoamphibole rocks worldwide (*e.g.*, Bachinski 1978, Schumacher 1988, Dymek & Smith 1990, Smith *et al.* 1992a, b, Pan & Fleet 1995, Schandl *et al.* 1995, Zaleski & Peterson 1995, Araujo *et al.* 1996). This interpretation has been extended to some sapphirine-bearing, granulite-facies equivalents of cordierite – orthoamphibole rocks (Warren 1979, Wilson & Baksi 1983, Peck & Valley 1996). Reinhardt (1987) proposed an alternative explanation for an occurrence of cordierite – orthoamphibole rocks in Queensland (Australia); he assigned a Mg-rich pelitic protolith to them. That occurrence is characterized by lower Fe and markedly different trace-element abundances than most other cordierite – orthoamphibole rocks.

The low variance of mineral assemblages in cordierite – orthoamphibole rocks make these rock types ideal candidates for petrological determination of metamorphic pressures and temperatures (Robinson *et al.* 1982). However, the abundance of cordierite and biotite in cordierite – orthoamphibole rocks allows diffusion of oxygen at low temperatures and make these rocks poor prospects for oxygen isotope thermometry; slow cooling will cause retrograde intermineral exchange of oxygen, such that peak-temperature isotope fractionations are unlikely to be preserved (*e.g.*, Eiler *et al.* 1993). Although thermometry using oxygen isotope fractionations is hampered by these properties, modeling of retrograde diffusion of oxygen can allow us to evaluate whether these rocks acted as closed systems after the peak of metamorphism, and can allow us to constrain the thermal history of these rocks.

In this study, we use oxygen isotope ratios of mineral separates from cordierite – gedrite rocks from the Central Metasedimentary Belt boundary thrust zone in the Grenville Province of Ontario to constrain the protolith and thermal history of these lithologies, as well as the nature of retrograde exchange of oxygen isotopes (*i.e.*, closed *versus* open system).

GEOLOGICAL SETTING

The Mid-Proterozoic Central Metasedimentary Belt boundary thrust zone (CMBbtz) is the southeast-dipping ductile shear zone that separates the Central Gneiss Belt (CGB) from the Central Metasedimentary Belt (CMB) in the Grenville Province of Ontario (Fig. 1). The Central Gneiss Belt is dominated by 1.7–1.4 Ga upper-am-

phibolite- and granulite-facies orthogneiss with minor paragneiss (Easton 1992), and has been subdivided on the basis of rock types, metamorphism, and structural style (*e.g.*, Davidson 1984). In Ontario, the Central Metasedimentary Belt is divided into the Frontenac and Elzevir terranes, and is bounded on the northwest by the CMBbtz. The Frontenac terrane is made up of granulite-facies marble, quartzite, pelites, and quartzofeldspathic gneiss, and is intruded by granitic plutons. The Elzevir terrane contains greenschist- to amphibolite-facies metasedimentary and *ca.* 1.29–1.24 Ga meta-volcanic rocks, intruded by suites of gabbroic, tonalitic, and granitic plutons (Easton 1992). Elements of the Elzevir terrane have been interpreted as both juvenile oceanic island arcs accreted on the southeastern margin of Laurentia (*e.g.*, Brown *et al.* 1975, Windley 1989) and as rifting and back-arc environments underlain by continental crust (*e.g.*, Smith & Holm 1990a, b, Smith & Harris 1996, Pehrsson *et al.* 1996, Smith *et al.* 1997).

The CMBbtz is characterized by gneissic thrust sheets of varying composition separated by anastomosing mylonitic and marble *mélange* tectonites (Hanmer 1988, Hanmer & McEachern 1992, McEachern & van Breemen 1993; see Fig. 2). Deformation in the thrust zone is first recorded at *ca.* 1.19 Ga and was renewed in the period 1.08–1.06 Ga (McEachern & van Breemen 1993). It is uncertain whether imbrication of the Central Metasedimentary Belt occurred at ~1.19 Ga (McEachern & van Breemen 1993) or at ~1.08 Ga (Timmermann *et al.* 1997). Pehrsson *et al.* (1996) proposed that the Raglan gabbro belt (Fig. 2) could have provided a rheologically stiff layer that determined the location of the top of the thrust zone. The lower boundary of the thrust zone is considered to be controlled by the presence of a relatively weak horizon of schistose aluminous gneisses (Hanmer 1988, Hanmer & McEachern 1992), including the cordierite – gedrite gneisses that are the focus of this study.

Cordierite – gedrite gneisses

Cordierite – gedrite rocks from Fishtail Lake (Locality 1, Fig. 2) have been the subject of petrological studies by Lal & Moorhouse (1969) and by Lal (1969a, b). These rocks contain the assemblages almandine + cordierite + phlogopite + quartz + plagioclase + either gedrite or sillimanite. K-feldspar, zircon, and Fe–Ti oxides are minor constituents, and staurolite inclusions can be found in garnet. Cordierite – gedrite rocks also are found 5–20 km west of Fishtail Lake in association with the Redstone and Dysart thrust sheets (Localities 2, 3, 4, Fig. 2). The cordierite – gedrite rocks are in a unit that records a polymetamorphic history, with a syntectonic assemblage of sillimanite + garnet + cordierite + two feldspars + quartz, and a post-tectonic assemblage of gedrite + cordierite + kyanite + biotite + garnet (Hanmer 1988, 1989), as well as quartz + plagioclase + garnet segregations (Culshaw 1986). Peak

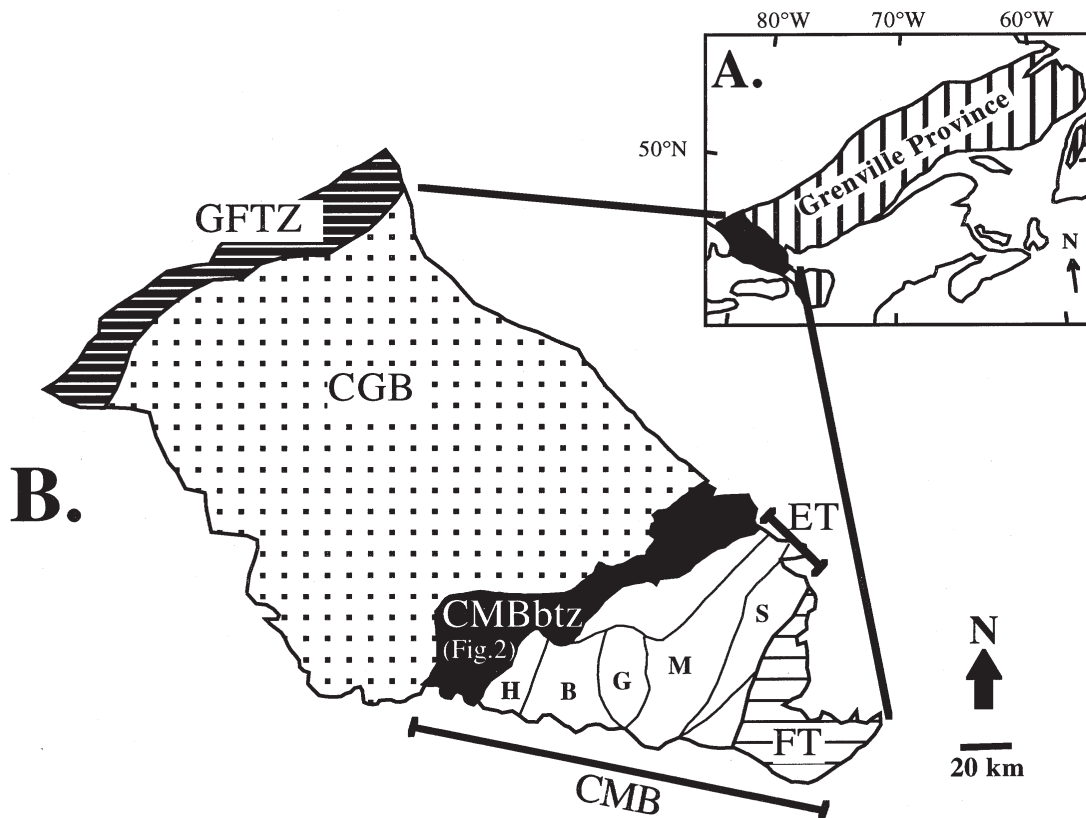


FIG. 1. A. Location map of the Grenville Province. B. The southern Grenville Province of Ontario, after Hanmer & McEachern (1992). GFTZ: Grenville Front Tectonic Zone, CGB: Central Gneiss Belt, CMBbtz: Central Metasedimentary Belt boundary thrust zone, ET: Elzevir terrane, FT: Frontenac terrane. The Elzevir terrane is subdivided into the Harvey – Cardiff (H), Belmont (B), Grimsthorpe (G), Mazinaw (M), and Sharbot Lake (S) domains, after Easton (1992).

temperatures and pressures of metamorphism for the southwestern part of the CMBbtz average 700°C and 8 kbar, as determined by a variety of independent thermometers and barometers (Anovitz & Essene 1990).

In the central and northern portion of the CMBbtz, outcrops of the cordierite – gedrite map unit are sparse (Hanmer & McEachern 1992), but are consistently found at the base of the thrust zone. The samples considered here from this region are from enstatite (En₇₀) + gedrite + cordierite + almandine gneisses from near Hoare Lake (Locality 5, Fig. 2) associated with enstatite-bearing migmatites (Millar 1983, Breaks & Thivierge 1985). This is the easternmost locality in which orthoamphibole has been identified, but aluminous rocks to the east have been correlated with this unit by lithologic similarity and structural position (Hanmer & McEachern 1992). Anovitz & Essene (1990) reported peak metamorphic temperatures and pressures of ~750°C and ~9 kbar from this area, similar to the ~800°C and ~8.9 kbar estimate of Carr & Berman (1997).

The protolith of these rocks is a subject of debate, and any model must explain the over 100 km strike-length of this unit along the base of the thrust zone. Proposed protoliths for these rocks include metamorphosed restites after partial melting (Lal & Moorhouse 1969, Breaks & Thivierge 1985), metamorphosed paleosols (Culshaw 1986), metamorphosed alkaline (phonolitic) volcanic rocks (perhaps including related sediments and metasomatized country-rock; see Easton 1992), and metamorphosed felsic volcanic rocks (Green & Smith 1996).

STABLE ISOTOPE ANALYSES

Analytical methods

Mineral separates (~2 mg per analysis) were hand-picked from crushed samples of cordierite – gedrite gneiss and related rock-types. Oxygen was liberated while heating with a CO₂ laser in the presence of BrF₅;

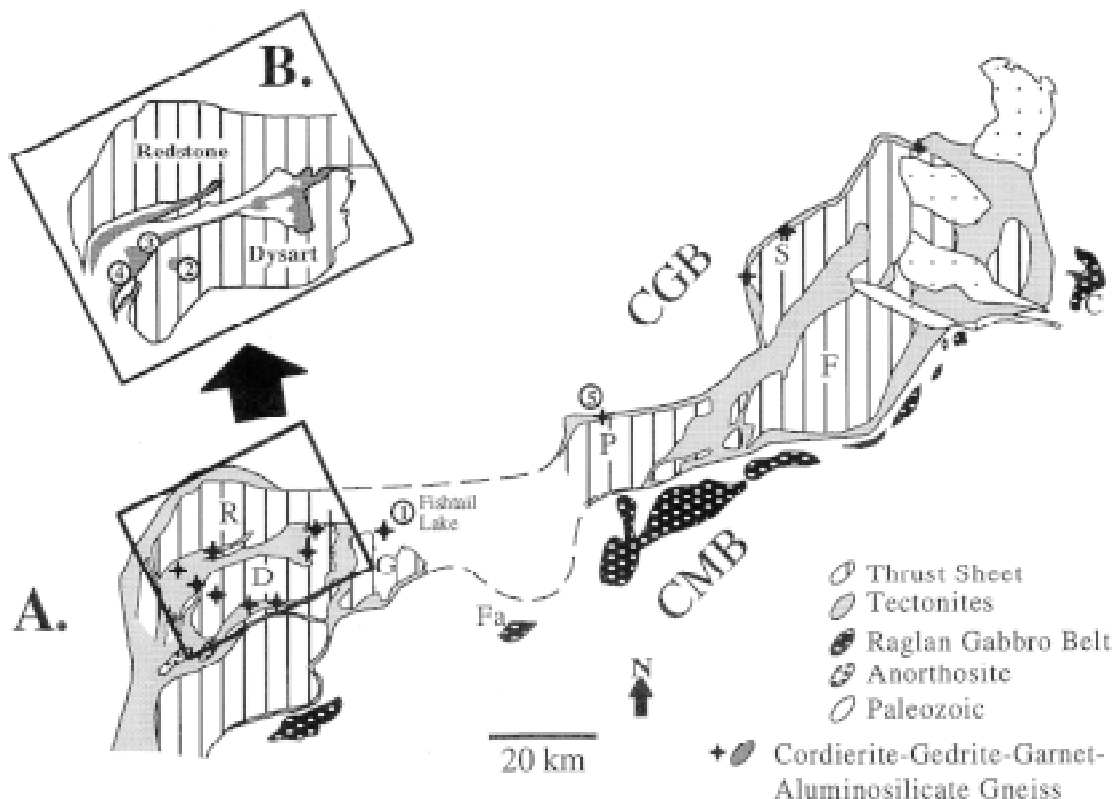


FIG. 2. A. Map of the Central Metasedimentary Belt boundary thrust zone after Hanmer & McEachern (1992). R: Redstone thrust sheet, D: Dysart thrust sheet, GL: Glamorgan thrust sheet, G: Grace thrust sheet, P: Papineau thrust sheet, F: Foymount thrust sheet, S: Stafford thrust sheet, F: Faraday Gabbro, C: Chenux Gabbro. B. Distribution of orthoamphibole – cordierite units around the Redstone and Dysart thrust sheets, after Hanmer (1988). Sample localities are shown and described in the text (Table 1).

Valley *et al.* (1995) described the analytical procedure in detail. Forty-three samples of garnet standard (UWG-2; Valley *et al.* 1995) were analyzed during ten days of analysis spread over a period of fourteen months. Analyses of UWG-2 yielded an average of $\delta^{18}\text{O}$ of $5.76 \pm 0.12\text{‰}$ ($1 \text{ sd} = 1$ standard deviation about the mean of the data). Uncertainty in the mean ($1\sigma = 1\text{sd}/n^{0.5}$) is 0.02‰ . These results are statistically indistinguishable from the long-term laboratory average for UWG-2 of $5.74 \pm 0.15\text{‰}$ ($n = 1081$, $1\sigma = 0.005\text{‰}$; Valley *et al.* 1995). Daily standard deviations of UWG-2 averaged 0.09‰ . NBS-28 African Glass Sand was analyzed on one analysis day and yielded a $\delta^{18}\text{O}$ value of $9.45 \pm 0.04\text{‰}$ ($n = 3$). The value of $\Delta_{\text{NBS28-UWG2}}$ was 3.58‰ , within 2 sd of the laboratory average of 3.70‰ (Valley *et al.* 1995). All oxygen isotope data are reported relative to Vienna Standard Mean Ocean Water (VSMOW).

Ninety-one mineral separates were analyzed for oxygen isotope ratio, and 47% of these analyses were duplicated or triplicated. Average reproducibility (half the difference between duplicate analyses or 1 sd of three

analyses) is as follows: quartz: 0.08‰ ($n = 11$), biotite: 0.09‰ ($n = 9$), amphibole: 0.09‰ ($n = 11$), garnet: 0.05‰ ($n = 11$). Analyses were adjusted by the amount the daily average $\delta^{18}\text{O}_{\text{UWG-2}}$ deviated from 5.8‰ , the accepted value of UWG-2 (Valley *et al.* 1995). The magnitude of this correction averaged 0.06‰ and was invariably less than 0.18‰ .

Results

Stable isotope analyses of mineral separates are compiled in Table 1. Two sample localities (1a and 1b) are from the two main lakeshore outcrops of cordierite – gedrite gneiss on the north shore of Fishtail Lake. Samples 96FL1 to 96FL12 (locality 1a) are from the easternmost cordierite – gedrite outcrop mapped by Lal & Moorhouse (1969), and samples 96FL13 to 96FL33 (locality 1b) are from the outcrop ~400 m to the west (see Fig. 1 in Lal & Moorhouse 1969). Analyses of spatially distinct hand-samples show little heterogeneity in $\delta^{18}\text{O}$ at each sample locality. Almandine from locality

TABLE 1. OXYGEN ISOTOPE RATIOS FOR SAMPLES FROM CORDIERITE–GEDRITE GNEISSES AND RELATED ROCKS, CENTRAL METASEDIMENTARY BELT BOUNDARY THRUST ZONE, ONTARIO

Sample	Assemblage	$\delta^{18}\text{O}$ Qtz	$\delta^{18}\text{O}$ Crd	$\delta^{18}\text{O}$ Bt	$\delta^{18}\text{O}$ Am	$\delta^{18}\text{O}$ Grt	$\delta^{18}\text{O}$ WR
Localities 1–5							
Fishtail Lake (Locality 1)							
96FL1	Qtz+Crd+Bt+Ged+Grt					5.39	6.7
96FL2	Qtz+Crd+Bt+Ged+Grt+Pl					5.75	
96FL3	Qtz+Crd+Bt+Ged					5.72	
96FL4	Qtz+Crd+Ged+Grt					5.86	
96FL5	Qtz+Bt+Ged+Grt+Pl					6.10	
96FL6	Qtz+Crd+Bt+Ged	6.75			5.83	5.79	7.1
96FL7	Qtz+Crd+Bt+Ged	6.75			5.83		
96FL9	Qtz+Bt+Ged+Grt+Pl					5.24	6.5
96FL10	Qtz+Bt+Crd+Grt+Sil					5.82	7.1
96FL11	Qtz+Crd+Bt	6.76	5.00	5.78			
96FL12	Qtz+Crd+Ged	6.41	4.51	6.51			
96FL13	Qtz+Crd+Bt+Grt+Pl	7.54			5.54	4.65	6.0
96FL14	Qtz+Crd+Bt+Ged+Grt	7.74				4.75	
96FL16	Qtz+Bt+Grt+Pl		4.52	4.86		4.65	6.2
96FL17	Qtz+Crd+Bt+Ged+Grt	8.46	4.58	4.69		4.96	6.0
96FL18	Qtz+Crd+Bt+Grt+Sil	8.47		5.46		4.82	6.1
96FL19	Qtz+Crd+Bt+Grt+Sil					4.77	
96FL20	Qtz+Crd+Bt+Grt+Sil					4.56	5.8
96FL21	Qtz+Bt+Grt+Pl	7.72				4.43	5.7
96FL22	Qtz+Bt+Ged	7.88				4.35	
96FL23	Qtz+Crd+Bt+Grt+Sil					5.18	6.5
96FL25	Qtz+Crd+Bt+Ged+Grt	9.15	4.33	5.26		5.26	6.5
96FL26	Qtz+Crd+Bt+Grt+Sil	9.02	4.57	5.27		5.27	
96FL27	Bt+Ged+Grt+Pl+Sil				5.16		
96FL28	Crd+Bt+Ged+Grt				5.04		
96FL29	Crd+Bt+Ged					4.38	5.7
96FL30	Qtz+Crd+Bt+Grt+Sil	7.39	4.58	5.03	4.93	4.93	6.1
96FL31	Qtz+Crd+Bt+Ged+Grt	7.67	4.83	5.10	4.78		
96FL32	Crd+Bt+Ged	7.50				4.43	5.7
96FL33	Qtz+Crd+Bt+Ged+Grt	7.63				4.41	
		7.41				4.47	
		8.13			5.35	4.46	5.8
		7.97			5.53	4.48	
						4.54	
						5.43	6.0
						5.37	6.6
						4.53	5.8
		9.53	4.99	6.10	5.00	6.3	
		9.34	5.08	6.43	5.04		
		9.16			5.19		
		9.10					
					5.25		
						4.60	5.9
Localities 6–14							
Localities 15–22							
Localities 23–25							
Localities 26–27							
Localities 28–29							
Localities 30–31							
Localities 32–33							
Localities 34–35							
Localities 36–37							
Localities 38–39							
Localities 40–41							
Localities 42–43							
Localities 44–45							
Localities 46–47							
Localities 48–49							
Localities 50–51							
Localities 52–53							
Localities 54–55							
Localities 56–57							
Localities 58–59							
Localities 60–61							
Localities 62–63							
Localities 64–65							
Localities 66–67							
Localities 68–69							
Localities 70–71							
Localities 72–73							
Localities 74–75							
Localities 76–77							
Localities 78–79							
Localities 80–81							
Localities 82–83							
Localities 84–85							
Localities 86–87							
Localities 88–89							
Localities 90–91							
Localities 92–93							
Localities 94–95							
Localities 96–97							
Localities 98–99							
Localities 100–101							
Localities 102–103							
Localities 104–105							
Localities 106–107							
Localities 108–109							
Localities 110–111							
Localities 112–113							
Localities 114–115							
Localities 116–117							
Localities 118–119							
Localities 120–121							
Localities 122–123							
Localities 124–125							
Localities 126–127							
Localities 128–129							
Localities 130–131							
Localities 132–133							
Localities 134–135							
Localities 136–137							
Localities 138–139							
Localities 140–141							
Localities 142–143							
Localities 144–145							
Localities 146–147							
Localities 148–149							
Localities 150–151							
Localities 152–153							
Localities 154–155							
Localities 156–157							
Localities 158–159							
Localities 160–161							
Localities 162–163							
Localities 164–165							
Localities 166–167							
Localities 168–169							
Localities 170–171							
Localities 172–173							
Localities 174–175							
Localities 176–177							
Localities 178–179							
Localities 180–181							
Localities 182–183							
Localities 184–185							
Localities 186–187							
Localities 188–189							
Localities 190–191							
Localities 192–193							
Localities 194–195							
Localities 196–197							
Localities 198–199							
Localities 200–201							
Localities 202–203							
Localities 204–205							
Localities 206–207							
Localities 208–209							
Localities 210–211							
Localities 212–213							
Localities 214–215							
Localities 216–217							
Localities 218–219							
Localities 220–221							
Localities 222–223							
Localities 224–225							
Localities 226–227							
Localities 228–229							
Localities 230–231							
Localities 232–233							
Localities 234–235							
Localities 236–237							
Localities 238–239							
Localities 240–241							
Localities 242–243							
Localities 244–245							
Localities 246–247							
Localities 248–249							
Localities 250–251							
Localities 252–253							
Localities 254–255							
Localities 256–257							
Localities 258–259							
Localities 260–261							
Localities 262–263							
Localities 264–265							
Localities 266–267							
Localities 268–269							
Localities 270–271							
Localities 272–273							
Localities 274–275							
Localities 276–277							
Localities 278–279							
Localities 280–281							
Localities 282–283							
Localities 284–285							
Localities 286–287							
Localities 288–289							
Localities 290–291							
Localities 292–293							
Localities 294–295							
Localities 296–297							
Localities 298–299							
Localities 300–301							
Localities 302–303							
Localities 304–305							
Localities 306–307							
Localities 308–309							
Localities 310–311							
Localities 312–313							
Localities 314–315							
Localities 316–317							
Localities 318–319							
Localities 320–321							
Localities 322–323							
Localities 324–325							
Localities 326–327							
Localities 328–329							
Localities 330–331							
Localities 332–333							
Localities 334–335							
Localities 336–337							
Localities 338–339							
Localities 340–341							
Localities 342–343							
Localities 344–345							
Localities 346–347							
Localities 348–349							
Localities 350–351							
Localities 352–353							
Localities 354–355							
Localities 356–357							
Localities 358–359							
Localities 360–361							
Localities 362–363							
Localities 364–365							
Localities 366–367							
Localities 368–369							
Localities 370–371							
Localities 372–373							
Localities 374–375							
Localities 376–377							
Localities 378–379							
Localities 380–381							
Localities 382–383							
Localities 384–385							
Localities 386–387							
Localities 388–389							
Localities 390–391							
Localities 392–393							
Localities 394–395							
Localities 396–397							
Localities 398–399							
Localities 400–401							
Localities 402–403							
Localities 404–405							
Localities 406–407							
Localities 408–409							
Localities 410–411							
Localities 412–413							
Localities 414–415							
Localities 416–417							
Localities 418–419							
Localities 420–421							
Localities 422–423							
Localities 424–425							
Localities 426–427							
Localities 428–429							
Localities 430–431							
Localities 432–433							
Localities 434–435							
Localities 436–437							
Localities 438–439							
Localities 440–441							
Localities 442–443							
Localities 444–445							
Localities 446–447							
Localities 448–449							
Localities 450–451							
Localities 452–453							
Localities 454–455							
Localities 456–457							
Localities 458–459							
Localities 460–461							
Localities 462–463							
Localities 464–465							
Localities 466–467							
Localities 468–469							
Localities 470–471							
Localities 472–473							
Localities 474–475							
Localities 476–477							
Localities 478–479							
Localities 480–481							
Localities 482–483							
Localities 484–485							
Localities 486–487							
Localities 488–489							
Localities 490–491							
Localities 492–493							
Localities 494–495							
Localities 496–497							
Localities 498–499							
Localities 500–501							
Localities 502–503							
Localities 504–505							
Localities 506–507							
Localities 508–509							
Localities 510–511							
Localities 512–513							
Localities 514–515							
Localities 516–517							
Localities 518–519							
Localities 520–521							
Localities 522–523							
Localities 524–525							
Localities 526–527							
Localities 528–529							
Localities 530–531							
Localities 532–533							
Localities 534–535							
Localities 536–537							
Localities 538–539							
Localities 540–541							
Localities 542–543							
Localities 544–545							
Localities 546–547							
Localities 548–549							
Localities 550–551							
Localities 552–553							
Localities 554–555							
Localities 556–557							
Localities 558–559							
Localities 560–561							
Localities 562–563							
Localities 564–565							
Localities 566–567							
Localities 568–569							
Localities 570–571							
Localities 572–573							
Localities 574–575							
Localities 576–577							
Localities 578–579							
Localities 580–581							
Localities 582–583							
Localities 584–585							
Localities 586–587							
Localities 588–589							
Localities 590–591							
Localities 592–593							
Localities 594–595							
Localities 596–597							
Localities 598–599							
Localities 600–601							
Localities 602–603							
Localities 604–605							
Localities 606–607							
Localities 608–609							
Localities 610–611							
Localities 612–613							
Localities 614–615							
Localities 616–617							

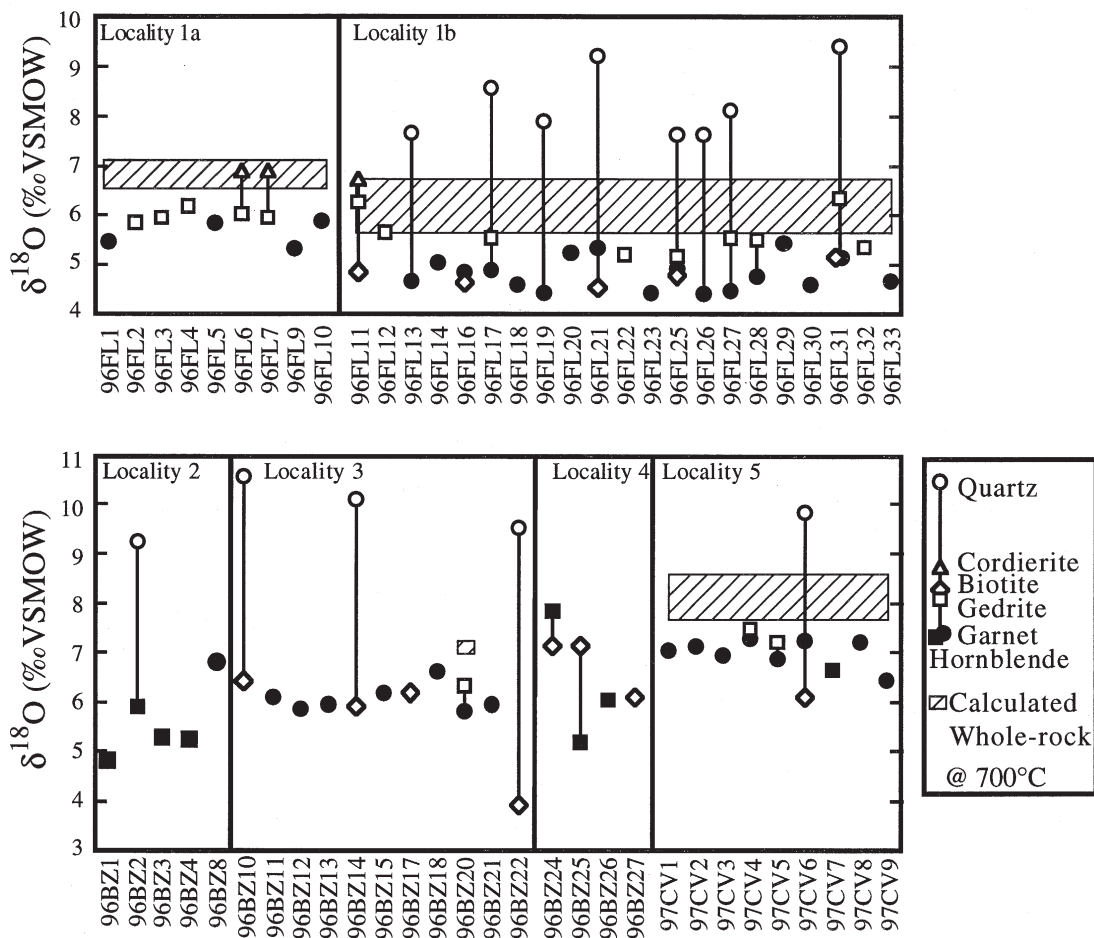


FIG. 3. Oxygen isotope ratios for mineral separates and calculated whole-rock values for localities 1–5. Mineral fractionations calculated at 700°C from data on equilibrium fractionation in Table 2 [and from Kohn & Valley (1998b) for hornblende] are shown for reference.

closure temperature of oxygen diffusion in almandine (Fig. 4), and almandine thus serves as an “inert marker” for isotopic fractionations during cooling.

Fractionations between quartz and almandine are well predicted by FGB diffusion modeling using “wet” diffusion data [experimentally determined at $P(\text{H}_2\text{O}) \approx 1$ kbar]; the average difference between modeled and measured $\Delta_{\text{Qtz-Alm}}$ is 0.2‰. If diffusion data from anhydrous experiments are used, the model underestimates the quartz – almandine fractionation by an average of 0.7‰. It is interesting to note that if high fugacities of H_2O in the “wet” experiments cause the faster diffusion of oxygen, the better match using “wet” data does not require the presence of H_2O as a free phase during metamorphism or during cooling. Anovitz & Essene (1990) estimated a P–T path of ~ 12 bar/°C for a sample from the CMBbtz north of Bancroft; thus for the $\sim 250^\circ\text{C}$ cool-

ing interval where quartz was open to exchange, the pressure ranged from 8 to 5 kbar. Even dry granulite-facies rocks (H_2O activities of 0.1 to 0.3) at 8 kbar have H_2O fugacities of ~ 1 to 2 kbar, comparable to those in “wet” oxygen diffusion experiments [$P(\text{H}_2\text{O}) = 1$ kbar, $f(\text{H}_2\text{O}) \approx 1$ kbar]. During metamorphism and cooling (from 700 to $\sim 550^\circ\text{C}$), H_2O activities in the cordierite – gedrite rocks from Fishtail Lake need only have been higher than ~ 0.1 to correspond to H_2O fugacities in “wet” experiments.

Reversed fractionations observed between phlogopite and almandine (Table 2) are predicted by modeling diffusive exchange using hydrothermal diffusion data, but would also be expected if oxygen diffusion in phlogopite were somewhat slower. Values of $\Delta_{\text{Ged-Alm}}$ calculated using hydrothermal diffusion data are lower than measured values, which are higher than equilibrium

TABLE 2. MEASURED AND PREDICTED OXYGEN ISOTOPE FRACTIONATIONS. PREDICTIONS ARE FROM FAST GRAIN BOUNDARY MODELING OF OXYGEN DIFFUSION

Diffusion Rates used	Hydrothermal (P _{H2O} =1kbar)						Dry
	ΔQz-Grt	ΔPl-Grt	ΔCrd-Grt	ΔGed-Grt	ΔPhl-Grt	ΔSil-Grt	
Equilibrium @700°C	2.70	1.47	0.80	0.52	0.40	0.30	2.70
96FL13 Model	3.24		-0.11		-1.81		2.80
96FL13 Measured	2.96		nd		nd		2.96
96FL17 Model	3.70		0.74	0.34	-0.90		2.74
96FL17 Measured	3.60		nd	0.61	nd		3.60
96FL19 Model	3.49		0.35		-1.32	-0.41	2.82
96FL19 Measured	3.41		nd		nd	nd	3.41
96FL21 Model	3.81	3.53	0.08		-1.66		2.84
96FL21 Measured	3.82	nd	nd		-0.81		3.82
96FL26 Model	3.31		0.13		-1.74	-0.57	2.88
96FL26 Measured	3.09		nd		nd	nd	3.09
96FL27 Model	3.51	4.61	0.62	0.17	-1.11	0.51	2.86
96FL27 Measured	3.56	nd	nd	0.95	nd	nd	3.56
96FL31 Model	3.50		0.78	0.16	-0.66		2.75
96FL31 Measured	4.21		nd	1.20	-0.04		4.21

nd, not determined; Modeling input parameters: peak temperature=700°C, cooling rate=2°C/M.y., all other input parameters are in Tables 3 and 4. Equilibrium fractionations @700°C (calculated from fractionation data in Table 3) are shown for reference.

values (Δ_{Ged-Alm} = 0.5‰ at 700°C: Kohn & Valley 1998b). This finding implies that during cooling, gedrite exchanged with some phase with a lower δ¹⁸O, pushing gedrite to higher values during cooling. If gedrite were to exchange primarily with phlogopite and not cordierite, then the δ¹⁸O values of gedrite would rise during cooling. Large values of Δ_{Ged-Alm} could be caused by the closure of cordierite to exchange earlier than it does in our models, a reasonable possibility, as oxygen diffusion in cordierite has not been experimentally determined and the value we use is an estimate (Table 3, Appendix 1).

The most important implication of diffusion modeling is the correlation of model and measured δ¹⁸O values for quartz and garnet, modally the most abundant

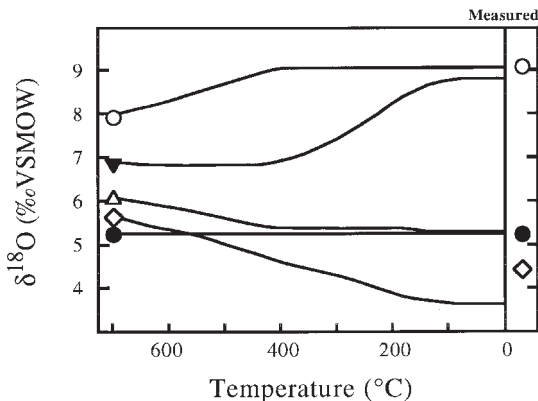


FIG. 4. Example of Fast Grain Boundary diffusion modeling (using diffusion data from hydrothermal experiments) for sample 96FL21. The left of the figure shows the equilibrium oxygen isotope fractionations at 700°C. The lines show the evolution of modeled δ¹⁸O values of minerals during cooling, and the right side of each figure shows the measured δ¹⁸O values for three minerals. Symbols as in Figure 1; inverted filled triangle: plagioclase.

mineral in the modeled Fishtail Lake samples. Diffusion rates and fractionation factors are well known for quartz and garnet, and their behavior provides information about the first ~250°C of cooling in these rocks. FGB diffusion modeling of oxygen exchange predicts the observed fractionations if we use “wet” oxygen diffusion data, peak metamorphic temperatures (Anovitz & Essene 1990) and cooling rates (Mezger *et al.* 1994) from the literature. Correspondence between observed and modeled values is best explained if samples were equilibrated at the peak of metamorphism, were dominated by diffusive transport of oxygen, and acted as closed systems to isotopically reactive external fluids for much of the cooling path.

WHOLE-ROCK δ¹⁸O VALUES

Interpretation of whole-rock oxygen isotope ratios in high-grade metamorphic rocks can be complicated by late-stage, low-temperature exchange (*i.e.*, retrogression, vein alteration, or weathering), which are undetectable if one analyzes only crushed rock. For this reason, we use δ¹⁸O values from minerals that are resistant to alteration to estimate the whole-rock δ¹⁸O at the peak of metamorphism. Almandine is the ideal mineral for this calculation because it forms below its blocking temperature in the rock types studied (Coghlan 1990), and should preserve a value of δ¹⁸O near peak conditions of metamorphism. The whole-rock δ¹⁸O value can then be calculated assuming that the observed modal minerals are representative of the minerals that were

TABLE 3. OXYGEN DIFFUSIVITIES AND EQUILIBRIUM OXYGEN ISOTOPE FRACTIONATIONS USED IN FAST GRAIN BOUNDARY DIFFUSION MODELING

Mineral	Q	D ₀	Reference	A	Reference
Quartz	243	2.90E-1	Farver & Yund (1991)	0	—
Quartz (dry)	221	2.10E-7	Dennis (1984)	0	—
Plagioclase	85	1.00E-9	Elphick <i>et al.</i> (1986)	1.15	Clayton <i>et al.</i> (1989)
Cordierite	107	4.50E-8	Giletti <i>et al.</i> (1978)	1.78	Hoffbauer <i>et al.</i> (1994)
Gedrite	163	2.00E-8	Farver & Giletti (1985)	2.05	Kohn & Valley (1998a)
Phlogopite	142	9.10E-6	Fortier & Giletti (1991)	2.16	Chacko <i>et al.</i> (1996)
Almandine	301	6.50E-5	Coghlan (1990)	2.55	Kohn & Valley (1998b)
Sillimanite	254.5	6.30E-7	Ghent & Valley (1998)	2.25	Sharp (1995)

Plagioclase is modeled as An₂₀. D₀ (pre-exponential factor in cm²s⁻¹) and Q (activation energy in kJ mol⁻¹) are from the Arrhenius relationship for the diffusion coefficient: D=D₀exp(-Q/RT) where R is the gas constant and T is temperature (K). All diffusion data are from hydrothermal experiments except the anhydrous (“dry”) experiments for oxygen diffusion in quartz of Dennis (1984). The Giletti *et al.* (1978) calibration for K-feldspar is used as a proxy for cordierite, and the Farver and Giletti (1985) calibration for tremolite is used for gedrite. A-factors are for the formula Δ_{Qt-Mineral}=A*10⁶/T².

present at the peak of metamorphism, but this does not require that the rest of the rock has acted as a closed system (with respect to oxygen) after that time. A drawback to this calculation is that garnet can grow over a range of temperatures along the prograde path. Fortunately, the difference between prograde fractionations and peak fractionations is small for most rock-types at high temperatures (Kohn 1993, Kohn *et al.* 1993). The average reproducibility of almandine analyses (predominantly single fragments of garnet) from single samples is $\pm 0.05\%$ ($n = 11$), suggesting that oxygen isotope inhomogeneity within single crystals is negligible. Whole-rock $\delta^{18}\text{O}$ values are calculated using values of $\delta^{18}\text{O}_{(\text{Alm})}$, oxygen isotope fractionation factors from Table 3, mineral modes from Table 4, and a peak temperature of 700°C (Anovitz & Essene 1990). The whole-rock $\delta^{18}\text{O}$ calculated is the whole-rock $\delta^{18}\text{O}$ at the time of peak metamorphism. The average calculated $\Delta_{(\text{WR-Alm})}$ is $1.27 \pm 0.34\%$ ($n = 7$); therefore calculated whole-rock $\delta^{18}\text{O}$ values from Fishtail Lake range from ~ 5.7 to 7.1% (Fig. 3). Sample 96BZ20, a similar rock-type from Locality 3, has a calculated whole-rock $\delta^{18}\text{O}$ of $\sim 7.1\%$, slightly higher than the average Fishtail Lake value. Rocks from Hoare Lake (locality 5) have calculated whole-rock $\delta^{18}\text{O}$ values between 7.6 and 8.4% . If the modal proportions of Lal & Moorhouse (1969) are used for this calculation, $\Delta_{(\text{WR-Alm})}$ is $1.45 \pm 0.23\%$ ($n = 7$), similar to the value calculated from our samples, but slightly higher because their samples are more quartz- and cordierite-rich.

TABLE 4. MODES AND GRAIN SIZES USED IN FAST GRAIN BOUNDARY MODELING OF OXYGEN DIFFUSION

	Qtz	Pl	Crd	Ged	Bt	Grt	Sil
96FL13							
Mode (%)	59		11		11	19	
Radius (mm)	0.4		0.2		0.5	1.1	
96FL17							
Mode (%)	17		33	22	9	19	
Radius (mm)	1.2		0.3	1.0	0.05	1.5	
96FL19							
Mode (%)	47		11		16	17	9
Radius (mm)	0.4		0.3		0.05	2.1	0.01
96FL21							
Mode (%)	41	15	4		31	9	
Radius (mm)	0.3	0.2	0.1		0.02	0.5	
96FL26							
Mode (%)	63		7		16	12	2
Radius (mm)	0.7		0.2		0.01	0.3	0.01
96FL27							
Mode (%)	49	1	1	1	31	14	3
Radius (mm)	0.3	0.1	0.1	1.0	0.07	1.0	0.01
96FL31							
Mode (%)	30		6	1	24	39	
Radius (mm)	1.0		0.4	1.5	0.05	2.0	

Modes were determined by counting 1000 points on thin sections. The average radius in thin section of quartz, feldspar, cordierite, and garnet was used; while the average radius along the C-axis was used for gedrite and biotite.

Whole-rock composition and $\delta^{18}\text{O}$ values allow us to exclude some proposed precursors of the cordierite – gedrite lithologies. Fe- and Al-rich lateritic soils typically have $\delta^{18}\text{O}$ values in near-equilibrium with local meteoric water at the low temperatures of weathering, resulting in values of $\sim 20\%$ (e.g., Giral *et al.* 1993). Mudrocks also have high $\delta^{18}\text{O}$ values, ranging from ~ 10 to $>20\%$, although values lower than 10% are observed (e.g., Land & Lynch 1996). Paragneisses from the Grenville Supergroup of Ontario have $\delta^{18}\text{O}$ values more typical of pelitic rocks, and average 14% (Shieh & Schwarcz 1978). Closed-system metamorphism of weathered horizons cannot explain the observed $\delta^{18}\text{O}$ values in the cordierite – gedrite rocks. The limited data on whole-rock compositions and trace-element concentrations in these rocks (Lal & Moorhouse 1969, Millar 1983, Breaks & Thivierge 1985, Culshaw 1986, Green & Smith 1996) also are inconsistent with pelitic sediments. Lal & Moorhouse (1969) proposed that removal of a granitic melt during metamorphism of pelitic sediments left a Fe- and Mg-rich restite, which new bulk composition led to the growth of cordierite + gedrite. Removal of 50% of a minimum-melt granitic fraction at 600°C leaving the bulk composition of the Fishtail Lake rocks would shift the restite to lower oxygen isotope ratios by $<0.5\%$; this process thus cannot account for the measured oxygen isotope compositions. The modally abundant quartz and the Ca-depletion in these rocks also are inconsistent with the restite hypothesis (Green & Smith 1996).

Hydrothermal alteration has the potential to either raise or lower $\delta^{18}\text{O}$ values of target rocks depending on the protolith $\delta^{18}\text{O}$, the source of fluids, and the temperature of alteration. If these cordierite – gedrite rocks represent hydrothermally altered rocks (subsequently metamorphosed), the temperature of alteration can only be estimated on the basis of oxygen isotope ratios if we know the protolith $\delta^{18}\text{O}$ and mineralogy, the $\delta^{18}\text{O}$ of the fluid, extent of exchange, and details of the flow system (*i.e.*, the scale of fluid permeability, temperature gradients, *etc.*). Modern basalt that has been hydrothermally altered on the seafloor displays heterogeneous alteration on the millimeter to meter scale, dominated by crack-controlled disequilibrium exchange (e.g., Thompson 1991). These heterogeneities would be variably smoothed by diffusion and exchange during amphibolite-facies metamorphism. Bulk chemical changes in basalt during intense hydrothermal alteration on the seafloor result in Ca-poor and Mg- and Al-rich compositions similar to most cordierite – gedrite rocks. In addition, both field and laboratory studies document similar compositional changes for intermediate and felsic volcanic rocks (Hajash & Chandler 1981, Shiraki *et al.* 1987, Thompson 1991). Assuming a mantle-like $\delta^{18}\text{O}_{(\text{whole-rock})}$ value of 6% and hydrothermal alteration with seawater ($\delta^{18}\text{O} \approx 0$), temperatures of exchange below $\sim 250^\circ\text{C}$ are required to produce higher $\delta^{18}\text{O}$ values (Cole *et al.* 1987), such as those observed. Whole-

rock $\delta^{18}\text{O}$ values of $\sim 7\text{‰}$ are common in the Mg- and Al-rich products of hydrothermal alteration of volcanic rocks (*e.g.*, Muehlenbachs 1986).

TECTONIC IMPLICATIONS

The protolith of the cordierite – gedrite gneisses in the CMBbtz is important because of their location at the base of the thrust zone, and their tectonic significance as an incompetent layer that controlled the location of the thrust zone (Hanmer 1988, Hanmer & McEachern 1992). Pehrsson *et al.* (1996) suggested that the CMBbtz is the site of closure of a marginal basin that developed above continental crust, as two bodies of gabbro from the Raglan Gabbro Belt (gabbros in Fig. 2a) contain inherited zircon with ages of 1.44–1.30 Ga, similar to ages found in the Central Gneiss Belt to the northwest. Only one fraction of inherited zircon comes from a body that is constrained to have crystallized before thrusting (the Chenaux gabbro, 1231 ± 2 Ma); other splits of inherited zircon are from the Faraday gabbro, for which the minimum age is 1165 Ma, younger than deformation and thrusting at ~ 1.19 Ga (McEachern & van Breemen 1993). These data are consistent with trace-element signatures of continental contamination in volcanic rocks from the Belmont domain (see Fig. 1, and Smith & Holm 1990a, b, Smith *et al.* 1997), interpreted as back-arc volcanic rocks formed above thinned continental crust. Smith & Harris (1996) used evidence of continental signatures in the Belmont domain as well as in arc volcanic rocks of the Mazinaw domain (Harnois & Moore 1991) to propose a tectonic model where the CMBbtz and Elzevir terrane are all underlain by contiguous continental crust prior to thrusting. In this model, the Mazinaw domain represents the ~ 1.2 Ga active arc southeast of Laurentia. The mafic–ultramafic succession in the southern Grimsthorpe domain (Easton & Ford 1994) is interpreted as an ophiolite sequence that formed as a small ocean basin in the back-arc.

The tectonic affinity of cordierite – gedrite rocks can be difficult to determine chemically because of mobility of major and trace elements during hydrothermal alteration. For example, at the Manitouwadge mining camp in Ontario, the cordierite – gedrite unit is interpreted (using data on the rare-earth elements) to result from hydrothermal alteration of a bimodal suite of volcanic rocks by seawater, now so extensively altered that they cannot be distinguished in the field (Pan & Fleet 1995). On the basis of SiO_2 content (Lal & Moorhouse 1969), the cordierite – gedrite unit from Fishtail Lake has andesitic to dacitic affinities, but altered volcanic rocks on the seafloor can undergo silicification or SiO_2 increase by mass loss (Thompson 1991). Trace-element geochemistry of immobile elements (see Green & Smith 1996), Nd isotope systematics, and detailed U–Pb geochronology of these rocks all have the potential to provide information concerning the petrogenesis of the igneous protolith.

We interpret these cordierite – gedrite gneisses as being metamorphosed hydrothermally altered volcanic rocks associated with Mid-Proterozoic rifting on the margin of Laurentia before 1.9 Ga. The consistency in style of hydrothermal alteration has resulted in similar and distinct bulk-compositions over a strike of over 100 km, comparable with the style of hydrothermal alteration on a system of spreading centers. It has been suggested that tectonic attenuation could contribute to the extensive strike-length of this unit as well as the distribution of alkaline rocks at the top of the CMBbtz (R.M. Easton, pers. commun., 1998). Although extension of the protolith is reasonable to expect in the thrust zone, the >100 km strike-length of this unit is well within the range of extent of ridge-style hydrothermal alteration. Since the cordierite – gedrite rocks are structurally between what has been interpreted as a back-arc environment underlain by continental crust (the CMBbtz and Belmont domain) and the margin of Laurentia, we favor a rift environment on the continental margin, similar to the tectonic environment of many volcanogenic massive sulfide deposits associated with continental rifts, which contain similar Mg- and Al-rich bulk compositions (Barrett & MacLean 1998). Thrust sheets in the CMBbtz are interpreted to have been thrust out-of-sequence (Hanmer 1988). Because of the relationship between thrust sheets and the cordierite – gedrite thrust zone tectonites (Hanmer & McEachern 1992), as well as the telescoped nature of the CMBbtz, we do not know the original geometry of the thrust sheets, the cordierite – gedrite rocks, the Central Gneiss Belt, and the Elzevir terrane. These constraints notwithstanding, it seems reasonable that if these rocks formed during rifting of the Laurentian Margin, then rifting occurred earlier than development of a marginal basin and arc volcanism to the east, as hypothesized by other investigators.

The well-studied Green Tuff belt of Japan, which hosts the Kuroko volcanogenic massive sulfide deposits, provides a useful Phanerozoic analog to these rocks, albeit in a slightly different tectonic environment. The Green Tuff belt is over 1,500 km long and ~ 100 km wide. It contains a package of hydrothermally altered Miocene volcanic and volcanoclastic rocks interpreted to be the result of aborted rifting of the Japan arc (Cathles *et al.* 1983). Hydrothermal alteration by seawater has resulted in zones with characteristic assemblages of minerals and styles of alteration. The most extreme alteration is in the “sericite” – chlorite zone, where rocks have low Ca and high Mg contents, and $\delta^{18}\text{O}_{(\text{whole-rock})}$ values are $6.7 \pm 1.3\text{‰}$ ($n = 31$, Green *et al.* 1983). If the Green tuff belt were metamorphosed to the upper amphibolite facies, it would become a package of diverse paragneiss, with only the Ca-poor “sericite” – chlorite zone becoming cordierite – orthoamphibole rocks. That the CMBbtz cordierite – gedrite rocks have similar $\delta^{18}\text{O}$ values from locality to locality is to be expected, because their distinctive bulk-

compositions were caused by the same style of hydrothermal alteration as their oxygen isotope compositions.

This model addresses the field relations and bulk-chemical and oxygen isotope compositions of the cordierite – gedrite unit, but also offers explanations of a number of observations in the literature. The differences in bulk-rock composition from different localities (Lal & Moorhouse 1969, Millar 1983, Breaks & Thivierge 1985, Culshaw 1986) could be the result of differences in local hydrothermal conditions or the alteration of different volcanic protoliths. A rifted continental margin would be expected to produce (variably contaminated) bimodal volcanism, and this is a possible explanation of the presence, in a sample from Fishtail Lake, of an enrichment in the light rare-earths (Green & Smith 1996). Easton (1987, 1992) noted an association of a rusty-weathering gneiss unit with high Sr, Y, Nd, and Zr contents with cordierite – gedrite rocks in the area of the Dysart thrust sheet, and concluded that the chemical composition and field relations of these rocks are consistent with alkaline volcanic rocks as a precursor. A continental rifting model is consistent with the generation of alkaline rocks, although trace-element mobility would be expected in the hydrothermal environment as well.

CONCLUSIONS

(1) A model of intermineral oxygen exchange in samples from Fishtail Lake yields values consistent with observed values. This agreement indicates that during cooling after the peak of metamorphism, these rocks were not infiltrated by large amounts of externally derived fluids.

(2) Mineral separates prepared from cordierite – gedrite rocks from the Central Metasedimentary Belt boundary thrust zone display consistent oxygen isotope systematics, yielding calculated whole-rock oxygen isotope ratios in the $\delta^{18}\text{O}$ range of 6–8‰. These calculated values are incompatible with either weathered material or pelitic metasedimentary rocks as a direct protolith of the cordierite – gedrite-bearing rock-types, even allowing for possible partial melting. The calculated values and whole-rock composition argue for a protolith consisting of volcanic rocks hydrothermally altered by seawater.

(3) We interpret the cordierite–gedrite-bearing rock-types as hydrothermally altered and metamorphosed volcanic remnants of rifting at the margin of Laurentia before development of a back-arc to the east.

ACKNOWLEDGEMENTS

This research was supported by DOE (93–ER14389) and NSF (EAR96–28260), with field support from the Weeks fund of the Department of Geology and Geophysics, University of Wisconsin – Madison. Matt Kohn supplied a copy of his modeling code for this study. We

thank Dave Farber and Mike DeAngelis for assistance in the field, Michael Easton for suggesting sampling localities, Brian Hess for making thin sections, and Mike Spicuzza for help and maintenance in the U.W. Stable Isotope Laboratory. Detailed reviews and comments by Michael Easton, Kurt Kyser, Bob Martin, and Michael Smith contributed to the clarity of presentation of data and ideas in this paper.

REFERENCES

- ANOVITZ, L.M. & ESSENE, E.J. (1990): Thermobarometry and pressure–temperature paths in the Grenville Province of Ontario. *J. Petrol.* **31**, 197–241.
- ARAUJO, S.M., SCOTT, S.D. & LONGSTAFFE, F.J. (1996): Oxygen isotope composition of alteration zones of highly metamorphosed volcanogenic massive sulfide deposits: Geco, Canada, and Palmeirópolis, Brazil. *Econ. Geol.* **91**, 697–712.
- BACHINSKI, D.J. (1978): Sulfur isotopic composition of thermally metamorphosed cupriferous iron sulfide ores associated with cordierite–anthophyllite rocks, Gull Pond, Newfoundland. *Econ. Geol.* **73**, 64–72.
- BARRETT, T. & MACLEAN, W. (1998): Volcanic sequences, litho geochemistry, and hydrothermal alteration in some bimodal volcanic-associated massive sulfide-systems. *In* Volcanic-Associated Massive Sulfide Deposits: Processes and Examples in Modern and Ancient Settings (C.T. Barrie & M.D. Hannington, eds.). *Rev. Econ. Geol.* **8**, 101–127.
- BREAKS, F.W. & THIVIERGE, R.H. (1985): Geology of the Wicklow area. *Ontario Geol. Surv., Open File Rep.* **5536**.
- BROWN, R.L., CHAPPELL, J.F., MOORE, J.M., JR. & THOMPSON, P.H. (1975): An ensimatic island arc and ocean closure in the Grenville Province of southeastern Ontario, Canada. *Geosci. Can.* **2**, 141–144.
- CARR, S. & BERMAN, R.G. (1997): Metamorphic history of the Bancroft – Barry’s Bay area, Ontario Grenville. *Geol. Assoc. Can. – Mineral. Assoc. Can., Program Abstr.* **22**, A-23.
- CATHLES, L.M., GUBER, A.L., LENAGH, T.C. & DUDÁS, F.Ö. (1983): Kuroko-type massive sulfide deposits of Japan: products of an aborted island-arc rift. *In* The Kuroko and Related Volcanogenic Massive Sulfide Deposits (H. Ohmoto & B.J. Skinner, eds.). *Econ. Geol., Monogr.* **5**, 96–114.
- CHACKO, T., HU, XIANGSHENG, MAYEDA, T.M., CLAYTON, R.N. & GOLDSMITH, J.R. (1996): Oxygen isotope fractionations in muscovite, phlogopite, and rutile. *Geochim. Cosmochim. Acta* **60**, 2595–2608.
- CHIBA, H., CHACKO, T., CLAYTON, R.N., & GOLDSMITH, J.R. (1989): Oxygen isotope fractionations involving diopside, forsterite, magnetite, and calcite: application to geothermometry. *Geochim. Cosmochim. Acta* **53**, 2985–2995.

- CLAYTON, R.N., GOLDSMITH, J.R. & MAYEDA, T.K. (1989): Oxygen isotope fractionation in quartz, albite, anorthite, and calcite. *Geochim. Cosmochim. Acta* **53**, 725-733.
- COLE, D.R., MOTTI, M.J. & OHMOTO, H. (1987): Isotopic exchange in mineral–fluid systems. II. Oxygen and hydrogen isotopic investigation of the basalt–seawater system. *Geochim. Cosmochim. Acta* **51**, 1523-1538.
- COGLAN, R.A.N. (1990): *Studies in Diffusional Transport; Grain Boundary Transport of Oxygen in Feldspars, Diffusion of Oxygen, Strontium and the REEs in Garnet, and Thermal Histories of Granitic Intrusions in South-Central Maine using Oxygen Isotopes*. Ph.D. thesis, Brown Univ., Providence, Rhode Island.
- CULSHAW, N.G. (1986): Geology of the Drag Lake area. *Ontario Geol. Surv., Open File Rep.* **5594**.
- DAVIDSON, A. (1984): Tectonic boundaries within the Grenville Province of the Canadian Shield. *J. Geodynamics* **1**, 433-444.
- DENNIS, P.F. (1984): Oxygen self diffusion in quartz. *Progress in Experimental Petrology* **6**, 260-265.
- DYMEK, R.F. & SMITH, M.S. (1990): Geochemistry and origin of Archaean quartz–cordierite gneisses from the Gothåbsfjord region, West Greenland. *Contrib. Mineral. Petrol.* **105**, 715-730.
- EASTON, R.M. (1987): Geology of the Lochlin area, county of Haliburton. *Ontario Geol. Surv., Open File Rep.* **5678**.
- _____ (1992): The Grenville Province and the Proterozoic history of central and southern Ontario. In *Geology of Ontario* (P.C. Thurston, H.R. Williams, R.H. Sutcliffe & G.M. Stott, eds.). *Ontario Geol. Surv., Spec. Vol.* **4**, 715-904.
- _____ & FORD, F.D. (1994): Geology of the Grimsthorpe area. *Ontario Geol. Surv., Open File Rep.* **5894**.
- EDWARDS, K.J. & VALLEY, J.W. (1998): Oxygen isotope diffusion and zoning in diopside: the importance of water fugacity during cooling. *Geochim. Cosmochim. Acta* **62**, 2265-2277.
- EILER, J.M., BAUMGARTNER, L.P. & VALLEY, J.W. (1992): Intercrystalline stable isotope diffusion: a fast grain boundary model. *Contrib. Mineral. Petrol.* **112**, 543-557.
- _____, _____ & _____ (1994): Fast grain boundary; a Fortran-77 program for calculating the effect of retrograde interdiffusion of stable isotopes. *Comput. Geosci.* **20**, 1415-1434.
- _____, VALLEY, J.W. & BAUMGARTNER, L.P. (1993): A new look at stable isotope thermometry. *Geochim. Cosmochim. Acta* **57**, 2571-2583.
- ELPHICK, S.C., DENNIS, P.F. & GRAHAM, C.M. (1986): An experimental study of the diffusion of oxygen in quartz and albite using an overgrowth technique. *Contrib. Mineral. Petrol.* **92**, 322-330.
- FARVER, J.R. & GILETTI, B.J. (1985): Oxygen diffusion in amphiboles. *Geochim. Cosmochim. Acta* **49**, 1403-1411.
- _____ & YUND, R.A. (1991): Oxygen diffusion in quartz: dependence on temperature and water fugacity. *Chem. Geol.* **90**, 55-70.
- FORTIER, S.M. & GILETTI, B.J. (1989): An empirical model for predicting diffusion coefficients in silicate minerals. *Science* **245**, 1481-1484.
- _____ & _____ (1991): Volume self-diffusion of oxygen in biotite, muscovite, and phlogopite micas. *Geochim. Cosmochim. Acta* **55**, 1319-1330.
- GHEENT, E. & VALLEY, J.W. (1998): Oxygen isotope study of quartz–Al₂SiO₅ pairs from the Mica Creek area, British Columbia: implications for the recovery of peak metamorphic temperatures. *J. Metamorphic Geol.* **16**, 223-230.
- GILETTI, B.J., SEMET, M.P. & YUND, R.A. (1978): Studies in diffusion. III. Oxygen and feldspars: an ion microprobe determination. *Geochim. Cosmochim. Acta* **42**, 45-57.
- GIRAL, S., SAVIN, S.M., GIRARD, J.-P. & NAHON, D.B. (1993): The oxygen isotope geochemistry of kaolinites from lateritic profiles: implications for pedology and paleoclimatology. *Chem. Geol.* **107**, 237-240.
- GREEN, G.R., OHMOTO, H., DATE, J. & TAKAHASHI, T. (1983): Whole-rock oxygen isotope distribution in the Fukazawa–Kosaka area, Hokuroku District, Japan, and its potential application to mineral exploration. In *The Kuroko and Related Volcanogenic Massive Sulfide Deposits* (H. Ohmoto & B.J. Skinner, eds.). *Econ. Geol., Monogr.* **5**, 395-411.
- GREEN, J.D., JR. & SMITH, M.S. (1996): The cordierite – orthoamphibole rocks of Fishtail Lake, Ontario; a re-evaluation of the restite hypothesis. *Geol. Soc. Am., Abstr. Programs* **28**(7), A45-46.
- HAJASH, A. & CHANDLER, G.W. (1981): An experimental investigation of high-temperature interactions between seawater and rhyolite, andesite, basalt and peridotite. *Contrib. Mineral. Petrol.* **78**, 240-254.
- HANMER, S. (1988): Ductile thrusting at mid-crustal level, southwestern Grenville Province, Ontario. *Can. J. Earth Sci.* **25**, 1049-1059.
- _____ (1989): Geology, western part of the Central Metasedimentary Belt boundary zone, Grenville Province, Ontario. *Geol. Surv. Can., Map* **1688A**.
- _____ & MCEACHERN, S. (1992): Kinematical and rheological evolution of a crustal-scale ductile thrust zone, Central Metasedimentary Belt, Grenville Orogen, Ontario. *Can. J. Earth Sci.* **29**, 1779-1790.
- HARNOIS, L. & MOORE, J.M. (1991): Geochemistry of two metavolcanic arc suites from the Central Metasedimentary

- Belt of the Grenville Province, southeastern Ontario, Canada. *Can. J. Earth Sci.* **28**, 1429-1443.
- HOFFBAUER, R., HOERNES, S. & FIORENTINI, E. (1994): Oxygen isotope thermometry based on a refined increment method and its application to granulite-grade rocks from Sri Lanka. *Precamb. Res.* **66**, 199-220.
- KOHN, M.J. (1993): Modeling of prograde mineral $\delta^{18}\text{O}$ changes in metamorphic systems. *Contrib. Mineral. Petrol.* **113**, 249-261.
- _____ & VALLEY, J.W. (1998a): Oxygen isotope geochemistry of the amphiboles; isotope effects of cation substitutions in minerals. *Geochim. Cosmochim. Acta* **62**, 1947-1958.
- _____ & _____ (1998b): Effects of cation substitutions in garnet and pyroxene on equilibrium oxygen isotope fractionations. *J. Metamorphic Geol.* **16**, 625-639.
- _____ & _____ (1998c): Obtaining equilibrium oxygen isotope fractionation from rocks. Theory and examples. *Contrib. Mineral. Petrol.* **132**, 209-224.
- _____, _____, ELSENHEIMER, D. & SPICUZZA, M.J. (1993): Oxygen isotope zoning in garnet and staurolite: evidence for closed-system mineral growth during regional metamorphism. *Am. Mineral.* **78**, 988-1001.
- LAL, R.K. (1969a): Paragenetic relations of aluminosilicates and gedrite from Fishtail Lake, Ontario, Canada. *Lithos* **2**, 187-196.
- _____ (1969b): Retrogression of cordierite to kyanite and andalusite at Fishtail Lake, Ontario, Canada. *Mineral. Mag.* **37**, 466-471.
- _____ & MOORHOUSE, W.W. (1969): Cordierite-gedrite rocks and associated gneisses of Fishtail Lake, Harcourt Township, Ontario. *Can. J. Earth Sci.* **6**, 145-165.
- LAND, L.S. & LYNCH, F.L. (1996): $\delta^{18}\text{O}$ values of mudrocks: more evidence for an ^{18}O -buffered ocean. *Geochim. Cosmochim. Acta* **60**, 3347-3352.
- MATTHEWS, A. (1994): Oxygen isotope geothermometers for metamorphic rocks. *J. Metamorphic Geol.* **12**, 211-219.
- MCEACHERN, S.J. & VAN BREEMEN, O. (1993): Age of deformation within the Central Metasedimentary Belt boundary thrust zone, southwest Grenville orogen: constraints on the collision of the Mid-Proterozoic Elzevir terrane. *Can. J. Earth Sci.* **30**, 1155-1165.
- MEZGER, K., ESSENE, E.J., VAN DER PLUIJM, B.A. & HALLIDAY, A.N. (1993): U-Pb geochronology of the Grenville Orogen of Ontario and New York; constraints on ancient crustal tectonics. *Contrib. Mineral. Petrol.* **114**, 13-26.
- MILLAR, W.D. (1983): *Metamorphic Petrography of Cordierite - Gedrite - Orthopyroxene Rocks and their Associated Gneisses of the Papineau Lake Region, Bangor Township, Ontario*. B.S. thesis, Queen's Univ., Kingston, Ontario.
- MUEHLENBACHS, K. (1986): Alteration of the ocean crust and the ^{18}O history of seawater. In *Stable Isotopes in High Temperature Geological Processes* (J.W. Valley, H.P. Taylor, Jr. & J.R. O'Neil, eds.). *Rev. Mineral.* **16**, 425-444.
- PAN, YUANMING & FLEET, M.E. (1995): Geochemistry and origin of cordierite-orthoamphibole gneiss and associated rocks at an Archean volcanogenic massive sulphide camp: Manitouwadge, Ontario, Canada. *Precamb. Res.* **74**, 73-89.
- PECK, W.H. & VALLEY, J.W. (1996): The Fiskenaesset Anorthosite Complex: stable isotope evidence for shallow emplacement into Archean ocean crust. *Geology* **24**, 523-526.
- PEHRSSON, S., HANMER, S. & VAN BREEMEN, O. (1996): U-Pb geochronology of the Raglan gabbro belt, Central Metasedimentary Belt, Ontario: implications for an ensialic marginal basin in the Grenville Orogen. *Can. J. Earth Sci.* **33**, 691-702.
- REINHARDT, J. (1987): Cordierite-anthophyllite rocks from north-west Queensland, Australia: metamorphosed magnesian pelites. *J. Metamorphic Geol.* **5**, 451-472.
- ROBINSON, P., SPEAR, F.S., SCHUMACHER, J.C., LAIRD, J., KLEIN, C., EVANS, B.W. & DOOLAN, B.L. (1982): Phase relations of metamorphic amphiboles: natural occurrence and theory. In *Amphiboles: Petrology and Experimental Phase Relations* (D.R. Veblen & P.H. Ribbe, eds.). *Rev. Mineral.* **9B**, 1-217.
- SCHANDL, E.S., GORTON, M.P. & WASTENEYS, H.A. (1995): Rare earth element geochemistry of the metamorphosed volcanogenic massive sulphide deposits of the Manitouwadge mining camp, Superior Province, Canada: a potential exploration tool? *Econ. Geol.* **90**, 1217-1236.
- SCHUMACHER, J.C. (1988): Stratigraphy and geochemistry of the Ammonoosuc volcanics, central Massachusetts and southwestern New Hampshire. *Am. J. Sci.* **288**, 619-663.
- SEKI, Y. (1957): Petrological study of hornfels in the central part of the median zone of the Kitakami Mountainland, Iwate Prefecture. *Sci. Rep. Saitama Univ., Ser. B*, **2**, 307-373.
- SHARP, Z.D. (1995): Oxygen isotope geochemistry of the Al_2SiO_5 polymorphs. *Am. J. Sci.* **295**, 1058-1076.
- SHIEH, YUCH-NING & SCHWARCZ, H.P. (1978): The oxygen isotope composition of the surface crystalline rocks of the Canadian Shield. *Can. J. Earth Sci.* **15**, 1773-1782.
- SHIRAKI, R., SAKAI, H., ENDOH, M. & KISHIMA, N. (1987): Experimental studies on rhyolite- and andesite-seawater interactions at 300°C and 1000 bars. *Geochem. J.* **21**, 139-148.
- SMITH, M.S., DYMEK, R.F. & CHADWICK, B. (1992a): Petrogenesis of Archean Malene supracrustal rocks, NW Buksefjorden region, West Greenland: geochemical evidence for highly evolved Archean crust. *Precamb. Res.* **57**, 49-90.

- _____, _____ & SCHNEIDERMAN, J.S. (1992b): Implications of trace element geochemistry for the origin of cordierite–orthoamphibole rocks from Orijärvi, SW Finland. *J. Geol.* **100**, 545–559.
- SMITH, T.E. & HARRIS, M.J. (1996): The Queensborough mafic-ultramafic complex: a fragment of a Mesoproterozoic ophiolite? Grenville Province, Canada. *Tectonophys.* **265**, 53–82.
- _____, _____ & HOLM, P.E. (1990a): The geochemistry and tectonic significance of pre-metamorphic minor intrusions of the Central Metasedimentary Belt, Grenville Province, Canada. *Precamb. Res.* **48**, 341–360.
- _____, _____ (1990b): The petrogenesis of mafic minor intrusions and volcanics of the Central Metasedimentary Belt, Grenville Province, Canada: MORB and OIB sources. *Precamb. Res.* **48**, 361–373.
- _____, _____, DENNISON, N.M. & HARRIS, M.J. (1997): Crustal assimilation in the Burnt Lake metavolcanics, Grenville Province, southeastern Ontario, and its tectonic significance. *Can. J. Earth Sci.* **34**, 1272–1285.
- THOMPSON, G. (1991): Metamorphic and hydrothermal processes: basalt–seawater interaction. In *Oceanic Basalts* (P.A. Floyd, ed.). Van Nostrand Reinhold, New York, N.Y. (149–171).
- TIMMERMANN, H., PARRISH, R.R., JAMIESON, R.A. & CULSHAW, N.G. (1997): Time of metamorphism beneath the Central Metasedimentary Belt boundary thrust zone, Grenville Orogen, Ontario: accretion at 1080 Ma? *Can. J. Earth Sci.* **34**, 1023–1029.
- VALLANCE, T.G. (1967): Mafic rock alteration and isochemical development of some cordierite–anthophyllite rocks. *J. Petrol.* **8**, 84–96.
- VALLEY, J.W. & GRAHAM, C.M. (1996): Ion microprobe analysis of oxygen isotope ratios in quartz from Skye granite: healed micro-cracks, fluid flow, and hydrothermal exchange. *Contrib. Mineral. Petrol.* **124**, 225–234.
- _____, KITCHEN, N., KOHN, M.J., NIENDORF, C.R. & SPICUZZA, M.J. (1995): UWG–2, a garnet standard for oxygen isotope ratios: strategies for high precision and accuracy with laser heating. *Geochim. Cosmochim. Acta* **59**, 5523–5531.
- YARDLEY, B.W.D. & VALLEY, J.W. (1997): The petrologic case for a dry lower crust. *J. Geophys. Res.* **102**, 12173–12185.
- WARREN, R.G. (1979): Sapphirine-bearing rocks with sedimentary and volcanogenic protoliths from the Arunta Block. *Nature* **278**, 159–161.
- WILSON, A.F. & BAKSI, A.K. (1983): Widespread $\delta^{18}\text{O}$ depletion in some Precambrian granulites of Australia. *Precamb. Res.* **23**, 33–56.
- WINDLEY, B.F. (1989): Anorogenic magmatism and the Grenvillian Orogeny. *Can. J. Earth Sci.* **26**, 479–489.
- ZALESKI, E. & PETERSON, V.L. (1995): Depositional setting and deformation of massive sulphide deposits, iron-formation, and associated alteration in the Manitouwadge Greenstone Belt, Superior Province, Ontario. *Econ. Geol.* **90**, 2244–2261.

Received February 2, 1998, revised manuscript accepted November 1, 1998.

APPENDIX. THE “FAST GRAIN BOUNDARY” MODEL

The intermineral diffusion of oxygen and the resetting of oxygen isotope ratios during cooling are modeled using the Fast Grain Boundary (FGB) diffusion model of Eiler *et al.* (1992), using the code of Eiler *et al.* (1994) with modifications by Kohn & Valley (1998c). The FGB model assumes peak metamorphic equilibration on the scale of several grain diameters, diffusive exchange through the crystal lattice, rapid exchange of oxygen and isotopic equilibrium along grain boundaries, and simple geometries for mineral phases (Eiler *et al.* 1992, 1993). Predicted intermineral fractionations calculated using FGB modeling are not particularly sensitive to differences in starting temperatures ($\pm 50^\circ\text{C}$) or cooling rates ($\pm 1^\circ\text{C}/\text{M.y.}$). For instance, the Fast Grain Boundary model has been shown to be a robust method of predicting intermineral fractionations in slowly cooled granulite- and amphibolite-facies diopside-bearing marble (Edwards & Valley

1998). Eight samples from Fishtail Lake (locality 1b) were selected for FGB modeling, and modeling inputs are found in Tables 3 and 4. These samples were chosen because they are unlayered and free of petrographic evidence of retrograde reactions (Lal & Moorhouse 1969, Lal 1969b). A peak regional metamorphic temperature of 700°C (Anovitz & Essene 1990) and a cooling rate of $2^\circ\text{C}/\text{M.y.}$ (Mezger *et al.* 1993) were used for all model runs.

Fractionation data used in this study are a combination of results of experiments, calculations, and empirical studies. The *A* factor ($\Delta_{\text{Qtz} - \text{Mineral}} \approx A * 10^6/T^2$) for plagioclase is calculated for An_{20} , linearly extrapolating between the experimental *A* factors for anorthite and albite (Clayton *et al.* 1989). The *A* factor for phlogopite is taken from the experiments of Chacko *et al.* (1996) combined with the calcite – quartz experiments of Clayton *et al.* (1989). Cordierite fractionation relative

to quartz was calculated by Hoffbauer *et al.* (1994) using a modified “increment method”. The sillimanite – quartz fractionation is taken from the empirical study of Sharp (1995). Both experiments (*e.g.*, Matthews 1994) and empirical studies (*e.g.*, Kohn & Valley 1998b) have shown a pronounced effect of solid solution on oxygen isotope fractionation factors of Ca-poor garnet. For this reason, we use the empirical fractionation between Ca-poor, almandine – pyrope garnet and diopside from Kohn & Valley (1998a), combined with the diopside experiments of Chiba *et al.* (1989). If the fractionation factor for grossular (Matthews 1994) were used, the model results would be systematically ~0.5‰ different from those using fractionation data for a Ca-poor garnet. The *A* factor for gedrite – quartz is calculated from the average gedrite – hornblende and garnet – hornblende fractionations at 575°C (Kohn & Valley 1998a), using the Ca-poor garnet – quartz fractionation above.

Diffusion coefficients for oxygen have been experimentally determined under both “dry” and “wet” [$P(\text{H}_2\text{O}) \approx 1$ kbar] conditions for quartz (Farver & Yund 1991), and under hydrothermal conditions for plagioclase (Elphick *et al.* 1996), phlogopite [using the “biotite” of Fortier & Giletti (1991)], and almandine (Coghlan 1990). Ghent & Valley (1998) have estimated the “wet” diffusion coefficients for sillimanite using the “ionic porosity” method of Fortier & Giletti (1989). Diffusion coefficients and activation energies have not been experimentally determined for cordierite or gedrite, so we use experimentally determined “wet” diffusivity of K-feldspar (Giletti *et al.* 1978) as a proxy for cordierite (after Hoffbauer *et al.* 1994) and the “wet” diffusivity of tremolite (Farver & Giletti 1985) as a proxy for gedrite. Two sets of calculations were made, the first using diffusion data from “wet” experiments, and the second using diffusion data to correspond with anhydrous (“dry”) experiments (see below).

The importance of H_2O fugacity in influencing rates of diffusion of oxygen during retrograde exchange in natural samples was demonstrated by Edwards & Valley (1998). They examined the difference in oxygen isotope ratios between large and small crystals of diopside from Grenville marbles and demonstrated that variable isotopic resetting was consistent with variable fugacity

of H_2O during cooling. Here we take a different approach because, although experimental data do exist to model these rocks under “wet” conditions, they do not exist to model these rocks under dry conditions. Variations in grain size in cordierite – gedrite gneisses are also not sufficient to produce a significant fractionation between large and small grains.

Figure 4 shows schematically how the modeled bulk-mineral $\delta^{18}\text{O}$ changes during cooling after a peak metamorphic temperature of 700°C using data for “wet” diffusion. In the model, garnet is closed to isotopic exchange, and quartz is the first mineral to cease exchange with the rest of the rock (at ~400°C). In rocks with gedrite, it is the second mineral to cease exchange (at ~350°C). Amphibole-group minerals cease exchange at lower temperatures than quartz because they allow faster diffusion of oxygen in wet experiments (Farver & Giletti 1985). Amphiboles also show less dependence of oxygen diffusivity on H_2O fugacity than does quartz (Farver & Giletti 1985, Farver & Yund 1991); thus under anhydrous conditions, quartz should still cease exchange before gedrite. Sillimanite has low modal abundance ($\leq 2\%$) in all but one sample and allows relatively slow diffusion of oxygen, so that it will not appreciably influence the order of oxygen isotope closure in these rocks.

Calculations of retrograde exchange of oxygen under anhydrous conditions can be made, but only down to the temperature where quartz closes to diffusion. Above this temperature, the data for “wet” diffusion are used for other minerals (except quartz), but the model still simulates anhydrous conditions because garnet is already closed to diffusion, and the other minerals allow rapid diffusion. We cannot model diffusion after quartz has closed because, in the absence of experimental data for the anhydrous case, we cannot predict the low-temperature behavior of gedrite, cordierite, and biotite. For the “wet” diffusion models, the isotopic fractionations among all minerals can be predicted (Table 2), but for the “dry” diffusion models, only the fractionation between garnet and quartz is predicted; therefore only predicted values of $\Delta_{\text{Qtz-Alm}}$ can be used to compare results for “wet” and “dry” models.